Macroscopic Subkelvin Refrigerator Employing Superconducting Tunnel Junctions

Xiaohang Zhang, Peter J. Lowell, Brandon L. Wilson, Galen C. O'Neil, and Joel N. Ullom

Phys. Rev. Applied **4**, 024006 — Published 10 August 2015

DOI: 10.1103/PhysRevApplied.4.024006

Macroscopic Sub-Kelvin Refrigerator Employing Superconducting Tunnel Junctions*

Xiaohang Zhang,† Peter J. Lowell, Brandon L. Wilson, Galen C. O'Neil, and Joel N. Ullom‡
National Institute of Standards and Technology
325 Broadway, Boulder, Colorado, 80305, USA
(Dated: July 13, 2015)

In this paper, we demonstrate a general-purpose macroscopic refrigerator based on the transport of electrons through superconducting tunnel junctions. Our refrigerator is intended to provide access to temperatures below those achievable using pumped ^{3}He. The refrigerator is cooled by 96 Normal-metal/Insulator/Superconductor (NIS) junctions divided among three separate silicon substrates. The use of thin-film devices on different substrates shows the potential to achieve higher cooling powers by connecting NIS devices in parallel. Improving on previous work [1], we demonstrate a larger temperature reduction, a more robust mechanical suspension, and a new electromechanical heat switch that will make it easier to integrate our refrigerator into other cryostats. The electromechanical heat switch has a measured thermal conductance in the on state of 1.2 ± 0.3 μW/K at 300 mK and no measurable thermal conductance in the off state. We observe a temperature reduction from 291 mK to 233 mK and infer cooling to 228 mK on longer timescales. The cooled payload is a metal stage whose mass exceeds 150 g and with 28 cm^2 of area for attaching user-supplied devices. Using the product of the cooled mass and the temperature reduction as a performance metric, this work is a more than 10-fold advance over previous efforts.

PACS numbers: 74.50.+r, 07.20.Mc, 85.30.Mn

I. INTRODUCTION

Sub-Kelvin temperatures play a growing role in both applied and basic science. Low temperature detectors are now used in applications such as single photon detection [2], standoff passive imaging for concealed weapons detection [3], and nuclear materials analysis [4]. Low temperature detectors are also now used in searches for weakly interacting dark matter [5] and an inflationary epoch in the early universe [6]. However, sub-Kelvin refrigeration is still challenging, especially below the minimum boiling point of ^{3}He, which is about 300 mK.

Currently, temperatures below 300 mK are reached using adiabatic demagnetization or dilution refrigerators. These two types of coolers are capable and well-developed but also are significantly more complicated than technologies that can reach 300 mK, such as pumped ^{3}He. Therefore, the development of a compact, easy-to-use, and simple refrigeration technology to cool from 300 mK to lower temperatures is of considerable practical interest. One candidate technology is refrigeration using superconducting tunnel junctions [7].

Following the first publication of superconducting tunnel junction refrigerator concepts [8] and the first demonstration of heat transfer from a normal metal to a superconductor [9], significant progress has been made towards practical tunnel junction refrigerators over the last two decades. NIS refrigerators have demonstrated large electronic temperature reductions [10, 11] and large cooling powers [12, 13]. They have cooled bulk objects [14] and lithographically integrated detectors [15, 16]. Very recently, we have demonstrated a general-purpose refrigerator using NIS junctions where general-purpose refer to a refrigerator that can cool user-supplied payloads, different payloads at different times, and payloads that are coupled to the refrigerator at a time of the user's choosing [1]. However, our proof-of-principle refrigerator had limitations including a fragile suspended stage, a small area for payload attachment, the need for modification of the surrounding cryostat to accommodate a mechanical heat switch, and only modest temperature reduction. In the work of [1], a temperature reduction of 34 mK from launch temperatures near 300 mK was observed in a stage whose mass was about 25 g.

In this paper, we demonstrate a far more robust general-purpose refrigerator with a cold stage area of 28 cm^2. Additionally, our refrigerator has an integrated electromechanical heat switch that is actuated via two superconducting wires to simplify the integration of the refrigerator with other cryostats. When cooled with NIS junctions, we show the temperature of the stage is reduced from 291 mK to 228 mK, which is a significant improvement over previous results.

II. THEORY AND FABRICATION

In an NIS junction biased near the energy gap of the superconductor, the most energetic electrons in the normal metal preferentially tunnel to the superconducting electrode so that heat in the normal metal is pumped to the superconductor [9] (Fig. 1). In order to cool a

† Also at University of Colorado, Boulder; xiaohang.n.zhang@nist.gov
‡ joel.ullom@nist.gov

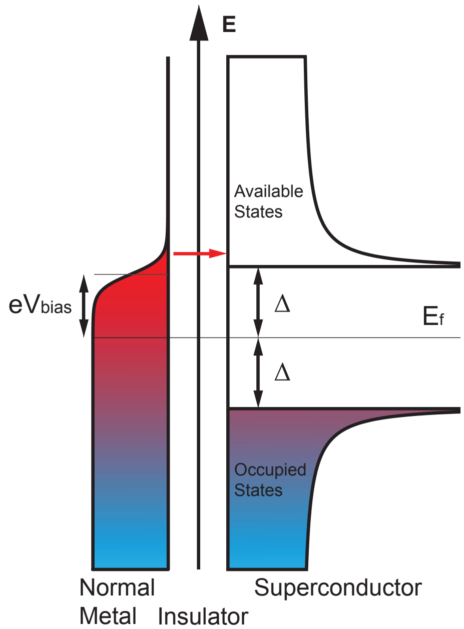

FIG. 1. (Color online) Density of states in an NIS tunnel junction. Occupied states are shaded from blue to red, where blue corresponds to low energy, and red corresponds high energy. When a voltage bias near 0.9 Δ/e is applied to the junction, the most energetic electrons in the normal metal will preferentially tunnel to the superconductor. This tunneling lowers the average energy of electrons in the normal metal, thus cooling its electron system.

galvanically isolated macroscopic stage, we have to cool phonons in the normal metal and in the stage, in addition to the electrons in the normal metal. Phonons in the normal metal can be cooled via the electron-phonon coupling in the film by extending the normal electrode onto a thermally isolated membrane. If the membrane is thin enough, phonons in the membrane will be decoupled from the phonons in the bulk substrate while remaining coupled to the cooled electrons [17]. After cooling the phonons in the membrane, we need to couple the cooled phonons to other objects such as the copper stage of our macroscopic refrigerator. To achieve this, we used gold wire bonds to connect a galvanically isolated metal film on the cooled membrane to the macroscopic stage. The NIS devices used in this work are the same devices used in previous experiments and are described elsewhere [1].

III. ROBUST COOLING STAGE AND ELECTROMECHANICAL HEAT SWITCH

One important component of this work is improvement of the cooling stage compared to our previous efforts [1]. Our first stage was highly susceptible to mechanical vibration such that routine movements in the surrounding laboratory produced measurable heating. Therefore, we built a new stage whose suspension system is based on

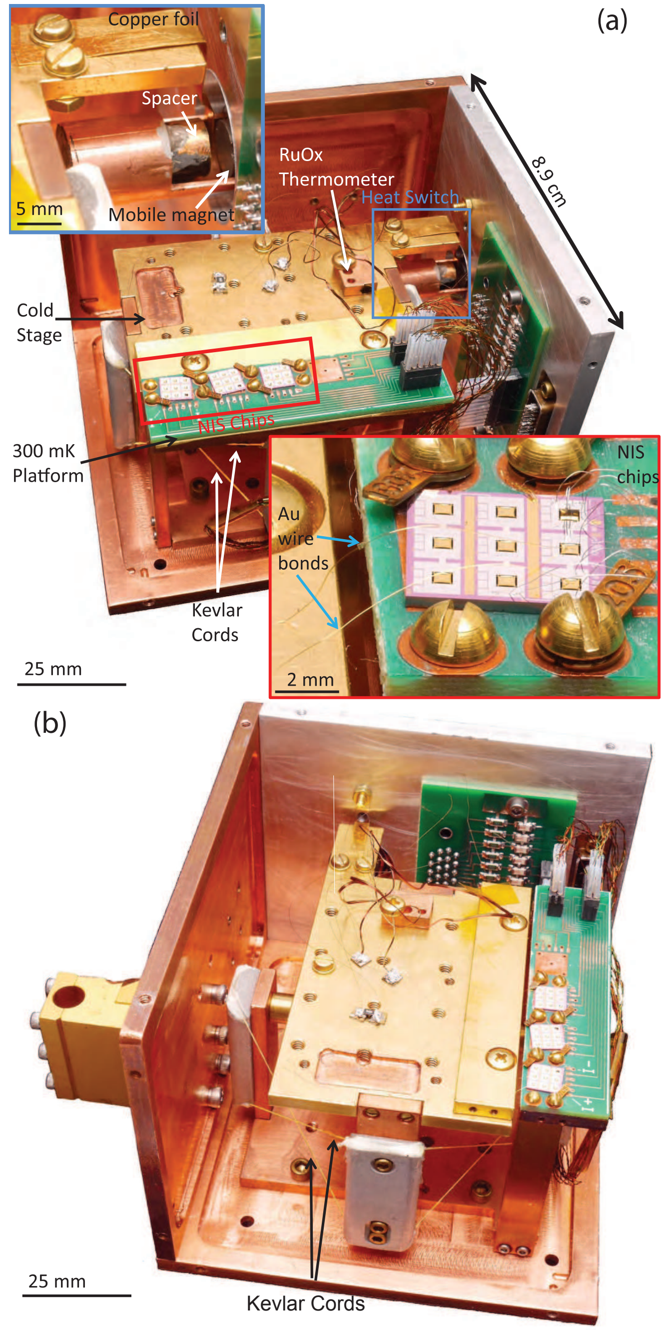

FIG. 2. (Color online) (a) Photograph of macroscopic refrigerator based on superconducting tunnel junctions. The Kevlar cords that isolate the macroscopic stage have been enhanced for clarity. The upper inset shows the electromagnetic heat switch that can connect the stage to the 300 mK bath. The lower inset shows at left the gold wire bond connections between the macroscopic stage and two NIS devices on one of three silicon substrates. Additional wire bonds on the right side of the lower inset carry electrical signals to and from the NIS devices. (b) A view of the macroscopic refrigerator from a second angle to show the Kevlar suspension and the separation of the suspended stage from the 300 mK platform containing the NIS devices. The Kevlar cords that isolate the macroscopic stage have been enhanced for clarity.

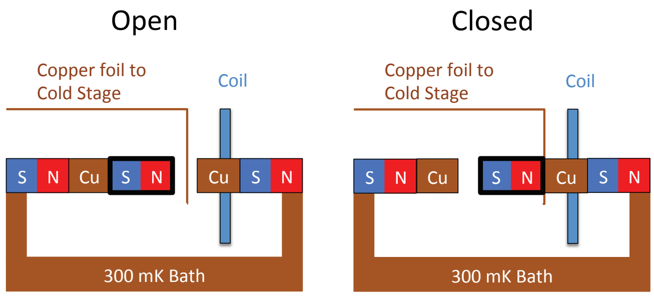

FIG. 3. (Color online) Diagram of electromechanical heat switch. The open state of the switch is shown at left, and the closed state at right. Blue and red rectangles represent the North (labeled N) and South (labeled S) poles of Sm-Co permanent magnets. One of the magnets, outlined in black is mobile. Copper parts are colored brown and/or labeled Cu. The thin brown line represents the gold plated copper foil attached to the cold stage. A superconducting coil (labeled and blue) is used to shift the position of the mobile magnet.

the designs of Roach [18]. The stage is suspended by eight Kevlar strands each with a 0.2 mm diameter and 5 cm in length. We chose Kevlar because it has a low thermal conductance while being structurally rigid when under tension. The stage deflected by only 25 µm under a vertical load of 2.5 kg.

The stage has a usable experimental area of 4.45 cm × 6.38 cm and consists of 125 g of oxygen-free high conductivity copper, 11 g of aluminum, and 17 g of brass. We made electrical connections to the stage using five Nb-Ti superconducting wires each with 40 µm diameter and about 20 cm length. The temperature of the stage was measured using a conventional ruthenium-oxide (RuOx) resistance thermometer.

Six Au wire bonds connect the stage to six NIS devices mounted on the warm side of the Kevlar suspension (see Fig. 2). The Au wire bonds are 25 µm in diameter and about 1 cm in length. We measured the thermal conductance G between the suspended stage and the frame with Kevlar, superconducting wires, and Au wire bonds connected to be 7.9 ± 0.1 nW/K [19] at 300 mK. By design, this G is low to enable cooling by the NIS junctions, so a heat switch is needed to increase the thermal conductance of the stage to the rest of our cryostat during precooling, for example from room temperature. However, the same switch must have a thermal conductance well below that of the Kevlar and wiring when in its off state.

In previous work, we used a heat switch that was actuated by pulling a fine cord that ran to room temperature. While this approach was successful, installation of such a cord into a new cryostat is a significant modification. Since our goal is the development of a self-contained NIS cooling module that can be easily integrated into other cryostats, we designed and built an electromechanical heat switch that can be actuated using electrical signals only. With such a heat switch, our improved macroscopic NIS refrigerator can be easily mounted to and operated within other cryostats.

The design of our electromechanical heat switch is related to that of a latching solenoid. As shown in Fig. 3, the heat switch consists of three permanent magnets with poles aligned. The location of the outer two magnets is fixed while the central magnet can slide within a copper tube between the fixed magnets. A fine copper wire attached to the central magnet provides heat sinking while permitting motion. The mobile magnet can latch to either of the two fixed magnets. The common axis of the three magnets is shared by a superconducting solenoid. Current flowing in the solenoid applies a force to the mobile magnet whose direction depends on the polarity of the current.

The electromechanical heat switch is mounted on the 300 mK shield of our refrigerator and a gold plated copper foil extends from the suspended stage to the space between the center and right-side magnets. One direction of current to the solenoid draws the central magnet to the right side of the switch, pinching the copper foil from the stage between the two magnets and closing the heat switch. The other direction of current pushes the central magnet to the left side of the switch, breaking contact to the copper foil and leaving the suspended stage thermally isolated. Hence, the physical principle that determines the on-state conductance is the attractive force between two permanent magnets.

The operating principle of the switch described here is significantly different compared to prior work. So-called gas-gap switches are widely used at very low temperatures [20, 21] but the walls that contain the gas volume have a finite off-state conductance that is typically too high for our application. Mechanical heat switches have near zero off-state conductance [22] but are often physically large and can dissipate too much energy when actuated for use at 300 mK. Heat switches based on the thermal conductivity variation of metal foils or wires between their normal and superconducting states have been used to obtain very high conductance ratios [23]. A superconducting switch based on a material with a transition temperature above 3 K to minimize its electronic thermal conductivity at 300 mK might be a candidate for our application but we did not pursue such an approach.

We used Samarium-Cobalt (SmCo) permanent magnets since they retain their magnetic moment at cryogenic temperatures better than many other types of rare-earth magnets [24, 25]. In order to keep the switch compact, we used cylindrical magnets with 6.35 mm diameter and 6.35 mm thickness. We measured the minimum force to separate the two magnets with a push-tip tension force gauge. The force required to separate the two magnets is about 1 N at room temperature. The solenoid was wound from 0.1 mm diameter insulated Nb-Ti superconducting wire with a Cu-Ni matrix. The solenoid has a length of 2.5 mm, an inner radius of 9.4 mm, an outer radius of 25 mm, and contained 1,200 turns of wire. A current of 70 mA through the solenoid was sufficient to push and pull the central magnet from one side of the switch to the other.

To determine the optimal location of the three magnets and the solenoid, we made a prototype heat switch where the spacing between components could be adjusted. From tests at room temperature, we determined a successful geometry and then fabricated a second switch where the component locations were set by the two copper spacers shown in Fig. 3. During room temperature operation, current needed to be supplied to the solenoid to change the state of the switch but not to maintain the switch in either the open or closed positions. However, we found during cryogenic operation that the central magnet was not stable in the open position unless 30 mA of current was kept in the solenoid. Because the solenoid was superconducting, this current did not dissipate power but a mature version of the switch would not require current in steady-state. Because the magnetization of SmCo changes with temperature, we believe the spacings determined at 300 K were not optimal for operation at 300 mK.

To test the reliability of the heat switch, we opened and closed it 1,000 times at 300 mK and observed that it operated properly each time. We measured if the switch was opened or closed by determining if there was a galvanic connection between the suspended stage and the rest of the cryostat. We measured the energy deposited at 300 mK from actuating the switch to be about 100 µJ [26]. We measured the thermal conductance of the heat switch by depositing power P on the suspended stage with the switch closed and recording the temperature difference ΔT between the stage and the surrounding heat bath. The thermal conductance G is given by $P/\Delta T$ so long as ΔT is much smaller than the 300 mK bath temperature. At 300 mK, our measured G is 1.2 ± 0.3 µW/K, which was suitable for our application. When the switch was open (off), the disappearance of the galvanic connection between the stage and the rest of the cryostat suggests the absence of a thermal pathway. The measured conductance between the stage and cryostat sets an extremely conservative upper bound on the off-state conductance of 7.9 ± 0.1 nW/K where this figure is dominated by the Kevlar, wiring, and connections to the tunnel junctions.

To compare our measured on-state conductance to historical data for pressed contacts, we used an expression for the thermal conductance of a pressed joint between two solids as a function of temperature, force, and contact material [27]. For 1 N and 300 mK, this expression predicts thermal conductances of 14.5 µW/K for gold-to-gold contacts and 0.7 µW/K for copper-to-copper contacts. We used gold-plated copper contacts and our results fall in between the predicted values. In the future, it may be possible to increase the G of the heat switch by using more powerful permanent magnets, by using current in the solenoid to increase the closing force, and by optimizing the choice of the contacting surfaces.

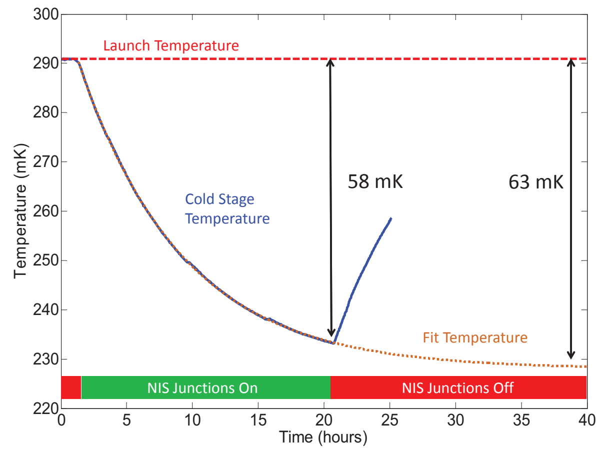

FIG. 4. (Color online) Temperature of the suspended stage measured by RuOx resistance thermometer versus time in hours. The solid blue line is the measured stage temperature, the dotted brown line is a fit to the temperature of the stage that is extended to show the ultimate base temperature of the experiment, and the dashed red line is the launch temperature of the refrigerator. The state of the NIS junctions is indicated at the bottom of the figure.

IV. COOLING PERFORMANCE

We measured the temperature reduction of the tunnel junction refrigerator in the following manner. First, we precooled our apparatus to about 300 mK using an Adiabatic Demagnetization Refrigerator (ADR). During precooling, the heat switch between the suspended stage and the surrounding heat bath was closed. Once the suspended stage temperature reached 291 mK, it was isolated from the rest of the cryostat by opening the heat switch and allowed to settle for an hour as shown in Fig 4. Then, we biased the refrigerator junctions for cooling. Cooling was performed using six separate tunnel junction refrigerator devices each with 16 junctions. The six devices were deposited on three separate silicon substrates. The bias current for the entire experiment was supplied using a single pair of wires because all the junctions were electrically connected in series. The optimal bias current of 2 µA was previously selected by finding the point on the current-voltage curves of the refrigerator junctions that showed the largest voltage enhancement in the subgap region which corresponds to the point of maximum cooling. The bias current was supplied using a battery in series with a 100 kΩ resistor. These results demonstrate the very modest infrastructure required to operate tunnel junction refrigerators.

While the internal temperature of the refrigerator junctions was determined using their current-voltage curves, the temperature of the suspended stage was directly and unambiguously measured by a RuOx resistance thermometer. After about 20 hours of cooling by the 96 junctions, the temperature of the suspended stage fell from 291 mK to 233 mK, a temperature reduction of

58 mK, which is a significant improvement over previous results [1]. Small features in the stage temperature of Fig. 4 at hours nine and 16 are due to vibrations from the transfer of liquid nitrogen into the surrounding cryostat.

After 20 hours, the cold heat capacity of the surrounding ADR was almost exhausted so we turned off the current bias to the junctions. As shown in Fig. 4, the temperature of the suspended stage then began to increase. It is clear from the shape of the curve in Fig. 4 that the stage had not yet reached its base temperature. While the cooling power of the junctions and the power loads on the stage have complex temperature dependencies, we are able to fit the cooling curve to the functional form,

$$T = a\, e^{-t/\tau} + b, \tag{1}$$

where T is temperature, t is time, and a, b, and τ are constant, in order to determine its asymptotic behavior. The results of the fit are also shown in Fig. 4 and indicate that the ultimate temperature is 228 mK, which is 63 mK colder than the launch temperature.

The ultimate temperature of 228 mK is warmer than expected. Based on previous measurements of the 16 junction subunits, we expected the temperature of the suspended stage would be reduced to 185 mK [28]. Since the base temperature of the cooling subunits is known as a function of applied power, we can deduce the power load on the stage and compare to the predicted load. The predicted load through the Kevlar and Nb-Ti wires is 218 pW when these connection span the temperature range 291 mK to 228 mK. Consequently, an additional power load of 684 pW is needed to account for the discrepancy between the expected and observed temperature reduction of the stage. The warm up rate of the stage after hour 20 is also consistent with an additional power load in this range.

Thermal models for NIS tunnel junction refrigerators are well established and balance the cooling power of the junctions against loads from electron-phonon coupling in the normal electrode, so-called quasiparticle backflow from the superconductor, Andreev currents, and hot phonons absorbed by device components on the membrane [29–33]. Coupling to a macroscopic stage introduces additional power loads from the mechanical and electrical connections to the stage. All of these terms are included in our power balance estimates. However, two power loads specific to the macroscopic stage are not included in thermal models to date. The first is long-term heat release from the epoxy on the suspended stage used to immobilize the Kevlar [23]. Since the ADR is periodically cycled to 4 K, the epoxy may never properly thermalize at the 291 mK launch temperature. The epoxy can be removed in the future. The second is power loading from the slow conversion of orthohydrogen to parahydrogen after cooling from 300 K. Molecular hydrogen in copper is known to precipitate into bubbles[23]. For a plausible but speculative H_2 concentration of 10 ppm, the estimated power load is within an order of magnitude of the observed value[34]. The stage copper can be heat treated in the future prior to assembly.

Another possible explanation is that the silicon block under one of the six NIS membranes touched the metal underneath. Ordinarily, the silicon blocks are several micrometers above the metal. However, the process of connecting the NIS devices to the stage or roughness on the metal surface could cause contact that results in an extra power load. Detailed modeling of tunnel junction refrigerators that are not attached to a macroscopic stage is in excellent agreement with data [11] so our present difficulties are clearly due to the stage. Improving agreement between the predicted and achieved temperature reduction is an important topic of future work.

We define the surplus cooling power as the power that can be added to the stage before the stage temperature rises 10 mK above its baseline value. Using this definition and including the mysterious 684 pW load, the surplus cooling power at the present 228 mK base temperature is calculated to be 189 pW. If the power load on the stage matched our predictions, then we calculate a surplus cooling power of 149 pW at a 185 mK base temperature. These cooling powers are low compared to other refrigerators such as ADRs and dilution refrigerators. However, the dissipation of typical cryogenic detectors, such as Transition Edge Sensors, is only about 10 pW per device. In addition, we have shown that more junctions can be attached in parallel to increase the cooling power.

Recent modeling of tunnel junction refrigerators like the ones used in this work predicts that technologically interesting temperature reductions are possible [35]. In particular, the modeling shows that a fully optimized macroscopic stage can be cooled from 300 mK to 100 − 110 mK. Looking farther into the future, related tunnel junction devices have recently demonstrated large electronic temperature reductions from launching temperature of 1 K and 100 mK [36, 37]. These results suggest that multi-stage tunnel junction refrigerators may be able to cool macroscopic payloads from near 1 K to below 100 mK.

V. CONCLUSION

In this paper, we demonstrate a thermally isolated and mechanically robust stage with an integrated electromechanical heat switch. The new mechanical suspension of the stage greatly reduces its susceptibility to mechanical vibrations from the outside environment. The new electromechanical heat switch operates on the principle of electrically induced magnetic latching and makes the integration of the stage into other cryostats significantly simpler by eliminating the need for a mechanical linkage to 300 K. The heat switch has a measured thermal conductance of 1.2 μW/K at 300 mK in the on state and no thermal conductance in the off state. We were able to operate the switch 1,000 times in a row without error. The stage provides an area of 28 cm^2 for other experiments.

We cooled the new stage using six discrete normal-metal/insulator/superconductor tunnel junction devices each with 16 junctions. The tunnel junction devices were distributed among three distinct silicon chips; these results clearly demonstrate the potential of NIS devices to provide increased cooling power when connected in parallel. The tunnel junction refrigerators were able to reduce the temperature of the stage from 291 mK to 228 mK and larger temperature reductions are anticipated in the future.

ACKNOWLEDGMENTS

This work is supported by the NASA Astrophysics Research and Analysis Program (APRA) and a National Research Council Postdoctoral Fellowship. We thank Douglas Bennett, Vincent Kotsubo, John Mates, and Daniel Schmidt for their technical assistance. We also thank Daniel Schmidt for the photographs used in this manuscript.

[1] Peter J Lowell, Galen C O'Neil, Jason M Underwood, and Joel N Ullom, "Macroscale refrigeration by nanoscale electron transport," Applied Physics Letters **102**, 082601 (2013).

[2] Robert H Hadfield, "Single-photon detectors for optical quantum information applications," Nature Photonics **3**, 696–705 (2009).

[3] Daniel T Becker, Cale Gentry, Ilya Smirnov, Peter A Ade, James A Beall, Hsiao-Mei Cho, Simon R Dicker, William D Duncan, Mark Halpern, Gene C Hilton, *et al.*, "Standoff passive video imaging at 350 GHz with 251 superconducting detectors," in *SPIE Defense+ Security* (International Society for Optics and Photonics, 2014) pp. 907804–907804.

[4] Michael W Rabin, "National and international security applications of cryogenic detectors-mostly nuclear safeguards," in *THE THIRTEENTH INTERNATIONAL WORKSHOP ON LOW TEMPERATURE DETECTORS LTD13*, Vol. 1185 (AIP Publishing, 2009) pp. 725–732.

[5] Z Ahmed, DS Akerib, S Arrenberg, CN Bailey, D Balakishiyeva, L Baudis, DA Bauer, PL Brink, T Bruch, R Bunker, *et al.*, "Dark matter search results from the CDMS II experiment." Science (New York, NY) **327**, 1619–1621 (2010).

[6] James Bock, Sarah Church, Mark Devlin, Gary Hinshaw, Andrew Lange, Adrian Lee, Lyman Page, Bruce Partridge, John Ruhl, Max Tegmark, *et al.*, "Task force on cosmic microwave background research," arXiv preprint astro-ph/0604101 (2006).

[7] Jukka Pekola, Robert Schoelkopf, and Joel Ullom, "Cryogenics on a chip," Physics Today **57**, 41–47 (2004).

[8] R. H. Parmenter, "Enhancement of superconductivity by extraction of normal carriers," Phys. Rev. Lett. **7**, 274–277 (1961).

[9] M Nahum, TM Eiles, and John M Martinis, "Electronic microrefrigerator based on a normal-insulator-superconductor tunnel junction," Applied Physics Letters **65**, 3123–3125 (1994).

[10] MM Leivo, JP Pekola, and DV Averin, "Efficient peltier refrigeration by a pair of normal metal/insulator/superconductor junctions," Applied physics letters **68** (1996).

[11] Galen C O'Neil, Peter J Lowell, Jason M Underwood, and Joel N Ullom, "Measurement and modeling of a large-area normal-metal/insulator/superconductor refrigerator with improved cooling," Physical Review B **85**, 134504 (2012).

[12] AM Clark, A Williams, ST Ruggiero, ML van den Berg, and JN Ullom, "Practical electron-tunneling refrigerator," Applied Physics Letters **84**, 625–627 (2004).

[13] Hung Q Nguyen, Matthias Meschke, and Jukka P Pekola, "A robust platform cooled by superconducting electronic refrigerators," Applied Physics Letters **106**, 012601 (2015).

[14] AM Clark, NA Miller, A Williams, ST Ruggiero, GC Hilton, LR Vale, JA Beall, KD Irwin, and JN Ullom, "Cooling of bulk material by electron-tunneling refrigerators," Applied Physics Letters **86**, 173508 (2005).

[15] NA Miller, GC O'Neil, JA Beall, GC Hilton, KD Irwin, DR Schmidt, LR Vale, and JN Ullom, "High resolution x-ray transition-edge sensor cooled by tunnel junction refrigerators," Applied Physics Letters **92**, 163501 (2008).

[16] N Vercruyssen, R Barends, Teunis Martien Klapwijk, JT Muhonen, M Meschke, and JP Pekola, "Substrate-dependent quasiparticle recombination time in superconducting resonators," Applied Physics Letters **99**, 062509 (2011).

[17] NA Miller, AM Clark, A Williams, ST Ruggiero, GC Hilton, JA Beall, KD Irwin, LR Vale, and JN Ullom, "Measurements and modeling of phonon cooling by electron-tunneling refrigerators," IEEE Transactions on Applied Superconductivity **15**, 556–559 (2005).

[18] Pat R Roach, "Kevlar support for thermal isolation at low temperatures," Review of Scientific Instruments **63**, 3216–3217 (1992).

[19] Using the peak-to-peak temperature measurement uncertainty as the temperature uncertainty, then use the error propagation formula to calculate the uncertainty of the G.

[20] I Catarino, G Bonfait, and L Duband, "Neon gas-gap heat switch," Cryogenics **48**, 17–25 (2008).

[21] DJ Frank and TC Nast, "Getter-activated cryogenic thermal switch," in *Advances in Cryogenic Engineering* (Springer, 1986) pp. 933–940.

[22] C Hagmann and PL Richards, "Adiabatic demagnetization refrigerators for small laboratory experiments and space astronomy," Cryogenics **35**, 303–309 (1995).

[23] Frank Pobell, *Matter and Methods at Low Temperatures* (Springer, Berlin, 2007).

[24] Rollin J. Parker and Robert J. Studders, *Permanent Magnets and Their Application* (John Wiley & Sons, New

York, 1962).

[25] D.L. Strnat and H. Mildrum, "High and low temperature properties of sintered Nd-Fe-B magnets," in *Proceedings of the 8th International Workshop on Rare Earth Magnets and Their Applications* (Dayton, Ohio, 1985).

[26] This number is calculated based on the heat capacity of the stage $C = 25$ mJ/K. Every time we operated the heat switch, the temperature of the suspended stage rose about 4 mK. Therefore the energy deposited from operating the switch is 25 mJ/K $\times$ 4 mK = 100 µJ.

[27] Jack W Ekin, *Experimental Techniques for Low-temperature Measurements* (Oxford Univ. Press, 2006).

[28] These measurements were conducted without the suspended stage. The membrane of each device contained a pair of NIS thermometer junctions and an Ohmic heater. By depositing power onto the membrane while running the refrigerator junctions on the substrate, we obtained detailed data on membrane temperature as a function of power load on the membrane. For a detailed discussion, please see Ref. [35].

[29] JN Ullom and PA Fisher, "Quasiparticle behavior in tunnel junction refrigerators," Physica B: Condensed Matter **284**, 2036–2038 (2000).

[30] Galen C O'Neil, Peter J Lowell, Jason M Underwood, and Joel N Ullom, "Measurement and modeling of a large-area normal-metal/insulator/superconductor refrigerator with improved cooling," Physical Review B **85**, 134504 (2012).

[31] Sukumar Rajauria, Philippe Gandit, Thierry Fournier, FWJ Hekking, Bernard Pannetier, and Hervé Courtois, "Andreev current-induced dissipation in a hybrid superconducting tunnel junction," Physical Review Letters **100**, 207002 (2008).

[32] Sukumar Rajauria, LMA Pascal, Ph Gandit, FWJ Hekking, Bernard Pannetier, and Hervé Courtois, "Efficiency of quasiparticle evacuation in superconducting devices," Physical Review B **85**, 020505 (2012).

[33] Juha T Muhonen, Matthias Meschke, and Jukka P Pekola, "Micrometre-scale refrigerators," Reports on Progress in Physics **75**, 046501 (2012).

[34] M Schwark, F Pobell, WP Halperin, Ch Buchal, J Hanssen, M Kubota, and RM Mueller, "Ortho-para conversion of hydrogen in copper as origin of time-dependent heat leaks," Journal of Low Temperature Physics **53**, 685–694 (1983).

[35] Peter J. Lowell, *Superconducting Tunnel Junction Refrigerators for Sub-Kelvin Cooling of Electrons, Phonons, and Arbitrary, User-Supplied Payloads.*, Ph.D. thesis, University of Colorado, Boulder (2014).

[36] Peter J Lowell, Galen C O'Neil, Jason M Underwood, Xiaohang Zhang, and Joel N Ullom, "Sub-100 mK cooling using normal-metal\insulator\superconductor tunnel junctions," Journal of Low Temperature Physics **176**, 1062–1068 (2014).

[37] O Quaranta, P Spathis, F Beltram, and F Giazotto, "Cooling electrons from 1 to 0.4 K with V-based nanorefrigerators," Applied Physics Letters **98**, 032501 (2011).